Article

Size-Dependent Phase Transformation Kinetics in Nanocrystalline ZnS

Feng Huang, and Jillian F. Banfield

J. Am. Chem. Soc., **2005**, 127 (12), 4523-4529• DOI: 10.1021/ja048121c • Publication Date (Web): 01 March 2005

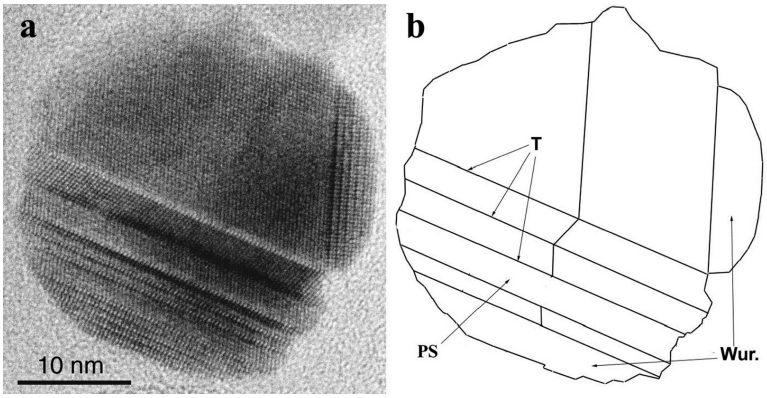

More About This Article

Additional resources and features associated with this article are available within the HTML version:

- Supporting Information
- Links to the 15 articles that cite this article, as of the time of this article download
- Access to high resolution figures
- Links to articles and content related to this article
- Copyright permission to reproduce figures and/or text from this article

View the Full Text HTML

J|A|C|S
ARTICLES
Published on Web 03/01/2005

Size-Dependent Phase Transformation Kinetics in Nanocrystalline ZnS

Feng Huang*,† and Jillian F. Banfield

Contribution from the Department of Earth and Planetary Science, University of California, Berkeley, and Lawrence Berkeley National Laboratory, Berkeley, California 94720-4767

Received January 16, 2005; E-mail: fhuang@fjirsm.ac.cn

Abstract: Nanocrystalline ZnS was coarsened under hydrothermal conditions to investigate the effect of particle size on phase transformation kinetics. Although bulk wurtzite is metastable relative to sphalerite below 1020 °C at low pressure, sphalerite transforms to wurtzite at 225 °C in the hydrothermal experiments. This indicates that nanocrystalline wurtzite is stable at low temperature. High-resolution transmission electron microscope data indicate there are no pure wurtzite particles in the coarsened samples and that wurtzite only grows on the surface of coarsened sphalerite particles. Crystal growth of wurtzite stops when the diameter of the sphalerite−wurtzite interface reaches ∼22 nm. We infer that crystal growth of wurtzite is kinetically controlled by the radius of the sphalerite−wurtzite interface. A new phase transformation kinetic model based on collective movement of atoms across the interface is developed to explain the experimental results.

Introduction

In bulk materials, the kinetics of transformation from one structure to another are difficult to determine. First-order, solid−solid-phase transitions often nucleate at defects, and thus the phase transformation rates are controlled by defect concentrations. As a transformed region of the crystal grows, mechanical forces may generate new defects, which in turn act as new nucleation sites. Because of the multiple nucleation events, the phase transition kinetics are complex.[1,2]

Nanometer-sized particles may offer important advantages for the study of phase transformation mechanisms. The kinetics of phase transitions in very small nanoparticles (3−5 nm) are usually simpler than those in bulk materials.[3,4] The temperature required to anneal out defects from nanoparticles is much lower than that in bulk materials;[4] thus, compared with bulk material, many small nanoparticles contain much less stable defects that could serve as nucleation sites for phase transformations.[3] However, if defects form in the initial stage of phase transformations due to thermal fluctuations, they only need to travel small distances to reach the surface. Consequently, phase transformations can propagate quickly through very small nanoparticles. Furthermore, since the propagation rate of a phase front across a very small nanoparticle is less than the time separation between successive nucleation events in one crystallite,[5−8] phase transitions in very small nanocrystals are usually single nucleation events.[3,4] In other words, once a defect such as a stacking fault forms in a very small nanoparticle, the energetic barrier for propagation of the new phase is small. The difficulty associated with moving a defect out of a nanoparticle will increase rapidly with increased particle size.

Although nanoparticles offer tractable systems for study of phase transformations in solids, the extent to which the results can be used to describe kinetics in bulk materials is uncertain. Thus, it is important to study phase transformations in nanoparticles and to determine the ways in which these depend on particle size and related factors. For example, nanoparticles can grow via oriented attachment (OA),[9,10] resulting in formation dislocations,[9] twins,[10] and stacking faults.[11] These defects can play important roles in subsequent reactions because they lower the energetic barriers for phase transformations relative to defect-free material.[10] Furthermore, completely different phase transformation mechanisms may be possible in small particles due to the small number of atoms involved.

The phase transformation of sphalerite (cubic ZnS) to wurtzite (hexagonal ZnS) in bulk material has been explained in terms of a periodic slip mechanism involving the expansion of stacking faults around an axial screw dislocation.[12−14] This mechanism may be fundamentally different to that operating in small particles. Previously, we demonstrated that OA introduces twins and stacking faults during crystal growth of nanocrystalline ZnS

† Current address: Fujian Institute of Research on the Structure of Matter, Chinese Academy of Sciences, Fujian, Fuzhou, 350002, P. R. China.

(1) Besson, J. M.; Itié, J. P.; Polian, A.; Weill, G.; Mansot, J. L.; Gonzalez, J. *Phys. Rev. B* **1991**, *44*, 4214.
(2) Venkateswaran, U. D.; Cui, L. J.; Weinstein, B. A. *Phys. Rev. B* **1992**, *45*, 9237.
(3) Chen, C.-C.; Herhold, A. B.; Johnson, C. S.; Alivisatos, A. P. *Science* **1997**, *276*, 398.
(4) Goldstein, A. N.; Echer, C. M.; Alivisatos, A. P. *Science* **1992**, *256*, 1425.
(5) Tolbert, S. H.; Alivisatos, A. P. *Annu. Rev. Phys. Chem.* **1995**, *46*, 595.
(6) Tolbert, S. H.; Alivisatos, A. P. *J. Chem. Phys.* **1995**, *102*, 4642.
(7) Tolbert, S. H.; Herhold, A. B.; Brus, L. E.; Alivisatos, A. P. *Phys. Rev. Lett.* **1996**, *76*, 4384.
(8) Zhang, H. Z.; Banfield, J. F. *J. Phys. Chem. B* **2000**, *104*, 3481.
(9) Penn, R. L.; Banfield, J. F. *Science* **1998**, *281*, 969.
(10) Penn, R. L.; Banfield, J. F. *Am. Mineral.* **1998**, *83*, 1077.
(11) Huang, F.; Zhang, H. and Banfield, J. F. *Nano Lett.* **2003**, *3*, 373.
(12) Daniels, B. K. *Philos. Mag.* **1966**, *14*, 487.
(13) Mardix, S.; Steinberger, I. T. *Isr. J. Chem.* **1966**, *3*, 243.
(14) Sebastian, M. T.; Krishna, P. *Pramana* **1984**, *23*, 395.

but does not yield pure wurtzite.[15,16] In this study, we report the kinetics of the phase transformation of sphalerite to wurtzite in relative big nanoparticles (typically ~30 nm in diameter). These are interesting because their sizes are large enough that the transformation mechanism characteristic of small nanoparticles becomes ineffective at some point in the growth of the new phase. Here we show that the formation of wurtzite is controlled by nucleation on the particle's surface and that growth of wurtzite into sphalerite is controlled by an energetic barrier that depends on the radius of the sphalerite−wurtzite interface.

Experimental Section

The mercaptoethanol-capped nanocrystalline ZnS used in this study was synthesized using Vogel's method.[17] Briefly, sodium sulfide aqueous solution was dropped into equal molar zinc chloride aqueous solution in the presence of 0.1 M mercaptoethanol at pH 10.2. Impurities were removed by dialysis treatment (until the pH was ~8.0 and Cl^- was below detection). The initial nanocrystalline ZnS product was coarsened in aqueous solution at 225 °C and 25 bar in hydrothermal bombs. For time series experiments, samples of the same batch of ZnS were coarsened in separate hydrothermal vessels and sacrificed for analysis after different periods of time. X-ray diffraction (XRD) was used to identify the phase composition and average particle sizes of initial and coarsened samples. Diffraction data were recorded using a Scintag PADV diffractometer with Cu Kα radiation (35 kV, 40 mA) in the step scanning mode. The 2θ scanning range was from 15° to 90° in steps of 0.02° with a collection time of 4 s per step. The average crystallite size was calculated from the peak broadening using the Scherrer equation. The phase composition of a sample can be calculated from the integrated intensities of the wurtzite (100) peak ($2\theta = 27.01$) and the overlapping sphalerite (111) and wurtzite (002) peaks ($2\theta = 28.64$). If the intensity ratio of wurtzite (100) to the overlapping peak is R, the weight fraction of wurtzite (F_w) can be calculated from

$$F_w = \frac{R}{I_w I_{ws} - R(I_{ws} - 1)} \quad (1)$$

where $I_w = 3.88$ represents the intensity ratio of the wurtzite (100) peak to the (002) peak, and $I_{ws} = 0.491$ is the intensity ratio of the wurtzite (002) peak to the sphalerite (111) peak.[18]

High-resolution transmission electron microscopy (HRTEM) was used to determine the particle morphology and for microstructure analysis and phase identification. Samples were prepared for HRTEM study by dispersing the ZnS powder onto holey carbon-coated Formvar supported by a copper mesh grid. HRTEM analyses were performed using a Philips CM200 UltraTwin HRTEM.

Results

As noted previously, crystal growth of mercaptoethanol-coated sphalerite under hydrothermal conditions occurs initially by OA and subsequently (after removal of the mercaptoethanol) by a combination of OA and Ostwald ripening.[11] In the later stages of crystal growth the particles become rounded, implying

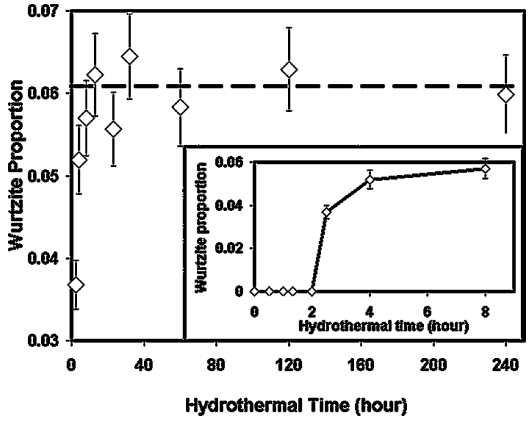

Figure 1. XRD-determined wurtzite proportion vs time at 225 °C. Inset is enlarged plot for the early coarsening stage.

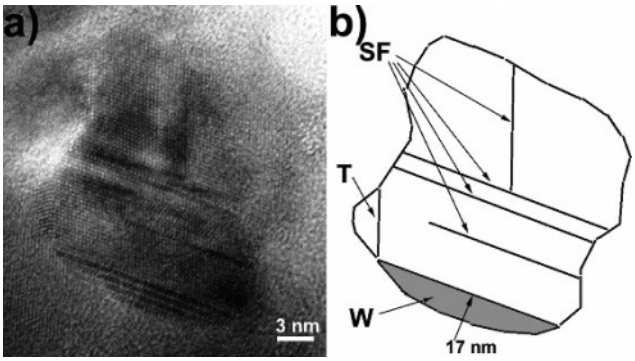

Figure 2. (a) HRTEM image of mercaptoethanol-capped ZnS samples coarsened at 225 °C for 4 h (very rare cases, larger particle). (b) Diagram illustrating the wurtzite (W) phase, position of stacking faults (SF), and twins (T) in the particle.

dominance of Ostwald ripening-based coarsening. X-ray diffraction phase compositional analysis shows that there is no detectable wurtzite (<1%) in the coarsened sample prior to the onset of Ostwald Ripening (2.5 h) (Figure 1 inset). Following the onset of Ostwald ripening, peaks in the XRD patterns indicate a sudden and sharp increase in wurtzite-like material, as of 3.7% content was detected at the first data point. (Note: From the XRD data it is not possible to determine whether these peaks are due to wurtzite or to closely spaced stacking faults, which introduce wurtzite-like structural elements.[19]) When the particle size is ~7 nm, the proportion of wurtzite-like material quickly reaches about 6% and remains constant, despite subsequent particle growth (Figure 1).

To evaluate the distribution of cubic and hexagonal ZnS and to identify the microstructures present, particles in coarsened samples were examined in zone axis orientations via HRTEM. TEM images were collected from samples taken after 0.5, 4, 32, and 120 h of coarsening. Most particles were 100% sphalerite. The sample coarsened for 4 h contained irregularly shaped sphalerite particles containing many twins and stacking faults, consistent with OA-based growth. Only in one case, wurtzite was found as a cap on the large sphalerite crystals surface over hundreds of measurements (Figure 2). The interface between sphalerite and wurtzite is about 17 nm. (Note: at this time point the wurtzite-like structure percentage is about 5.3%, not arrives the 6% saturated point; see Figure 1 inset.)

(15) Huang, F.; Zhang, H.; Banfield, J. F. *J. Phys. Chem. B* **2003**, *107*, 10470.
(16) There are many polytype stacking patterns possible in the close packed ZnS structure. In this article, we defined wurtzite as at least 3−4 layers of wurtzite type stacking: ...ABABAB... This cannot be generated via oriented attachment involving sphalerite or polytypically complex nanoparticles and is inferred to form by phase transformation.
(17) Vogel, W.; Borse, P. H.; Deshmukh, N.; Kulkarni, S. K. *Langmuir* **2000**, *16*, 2032.
(18) To obtain the coefficient of I_w and I_{ws}, we synthesized pure sphalerite and wurtzite bulk materials. We mixed two samples in weight proportion (F_w) of 0, 25, 50, 75, and 100% wurtzite and obtained the XRD intensity ratio of the wurtzite (100) peak and the peak (R) due to the combination of the sphalerite (111) and wurtzite (200) peaks. Fitting the experimental R versus F_w data with eq 1 and using I_w and I_{ws} as parameters, we obtain $I_w = 3.88$ and $I_{ws} = 0.491$.
(19) Huang, F.; Zhang, H.; Banfield, J. F., in preparation.

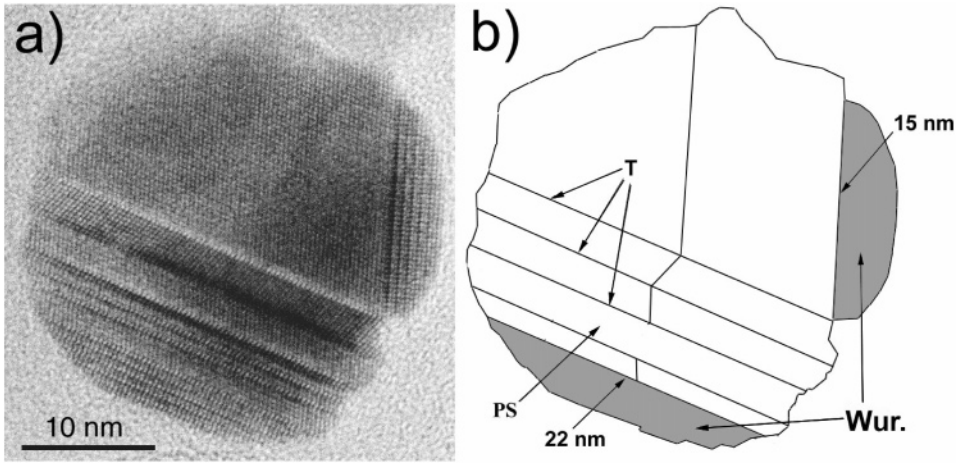

Figure 3. (a) Typical HRTEM image of mercaptoethanol-capped ZnS samples coarsened at 225 °C for 32 h. (b) Diagram illustrating the wurtzite (W) phase, polytype structure (PS), and position of twins (T) in the particle.

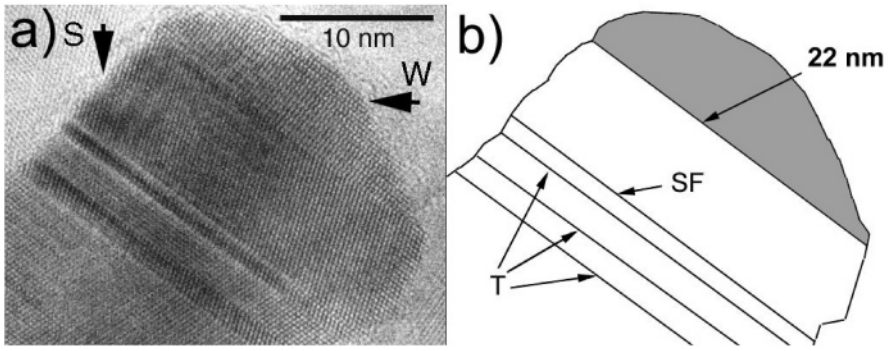

Figure 4. (a) Typical HRTEM image of mercaptoethanol-capped ZnS samples coarsened at 225 °C for 120 h. (b) Diagram illustrating the wurtzite (W) phase and positions of stacking faults (SF) and twins (T) in the particle.

Arround 90% of the particles in samples reacted for longer times (32 and 120 h) were sphalerite (measured from TEM observation), but wurtzite (several unit cells) was present on the surfaces of some cases. The partial transformation of sphalerite particles to wurtzite rather than formation of discrete wurtzite particles is consistent with the observation of highly anisotropic (non-Gaussian) XRD peaks (data not shown).

HRTEM images of 10 different nanoparticles in zone axis orientations were recorded for detailed analysis. Figures 3 and 4 are typical HRTEM images of mercaptoethanol-capped ZnS coarsened at 225 °C for 32 and 120 h, respectively. Wurtzite developed with (001) parallel to one or more {111} sphalerite surfaces (e.g., [001] wurtzite parallel to ⟨111⟩ sphalerite), as expected based on stacking considerations. Wurzite was never observed in zones within sphalerite crystals. Formation of wurtzite in our experiments (225 °C) at temperatures far below those needed to transform bulk sphalerite to wurzite (1020 °C) suggests that nanowurtzite becomes more stable than sphalerite in nanocrystalline ZnS at 225 °C.

When we compared the 10 HRTEM images taken at 32 and 120 h, we found that, with increasing coarsening time, the interface size between wurtzite and sphalerite does not change significantly, despite an increase in the average sphalerite diameter to >30 nm. In the most reacted samples, HRTEM images reveal that the diameters and areas of the interfaces between sphalerite and wurtzite are the same in all cases: about 22 and 380 nm^2, respectively. Only in the case when the wurtzite−sphalerite interface meet the twin structure, the interface size could be smaller, about 15 nm as shown in Figure 3.

Discussion

We observed transformation of sphalerite to wurtzite in nanoparticles of ZnS in hydrothermal solutions at 225 °C. This implies that nanoparticles of wurtzite are stable relative to sphalerite nanoparticles under these conditions. This result is consistent with MD predictions reported previously.[20]

The experimental data indicate that wurtzite forms only during the stage where coarsening occurs by a combination of OA and Ostwald ripening of sphalerite (2.5−13 h). However, the abundance of wurtzite does not continue to increase over long reaction times (Figure 1). It is possible to use this observation to show that wurtzite detected at the end of the experiment did not form on small particles that subsequently grew significantly via Ostwald ripening. If this occurred, the increase in the volume of wurtzite (Figure 5a) would be given by wurtzite % = $[3r - (r - 10.5295)](r - 10.5295)^2/4r^3$. For example, an initial 15-nm particle with 6% wurtzite would be converted to a 30-nm particle containing 24.8% wurtzite if the particle grows by addition of atoms to the surface, with the structure determined by the underlying polymorph.

Wurtzite regions could form in the interiors of crystals if growth occurred by OA involving wurtzite or wurtzite and

(20) Zhang, H.; Huang, F.; Gilbert, B.; Banfield, J. F. *J. Phys. Chem. B* **2003**, *107*, 13051

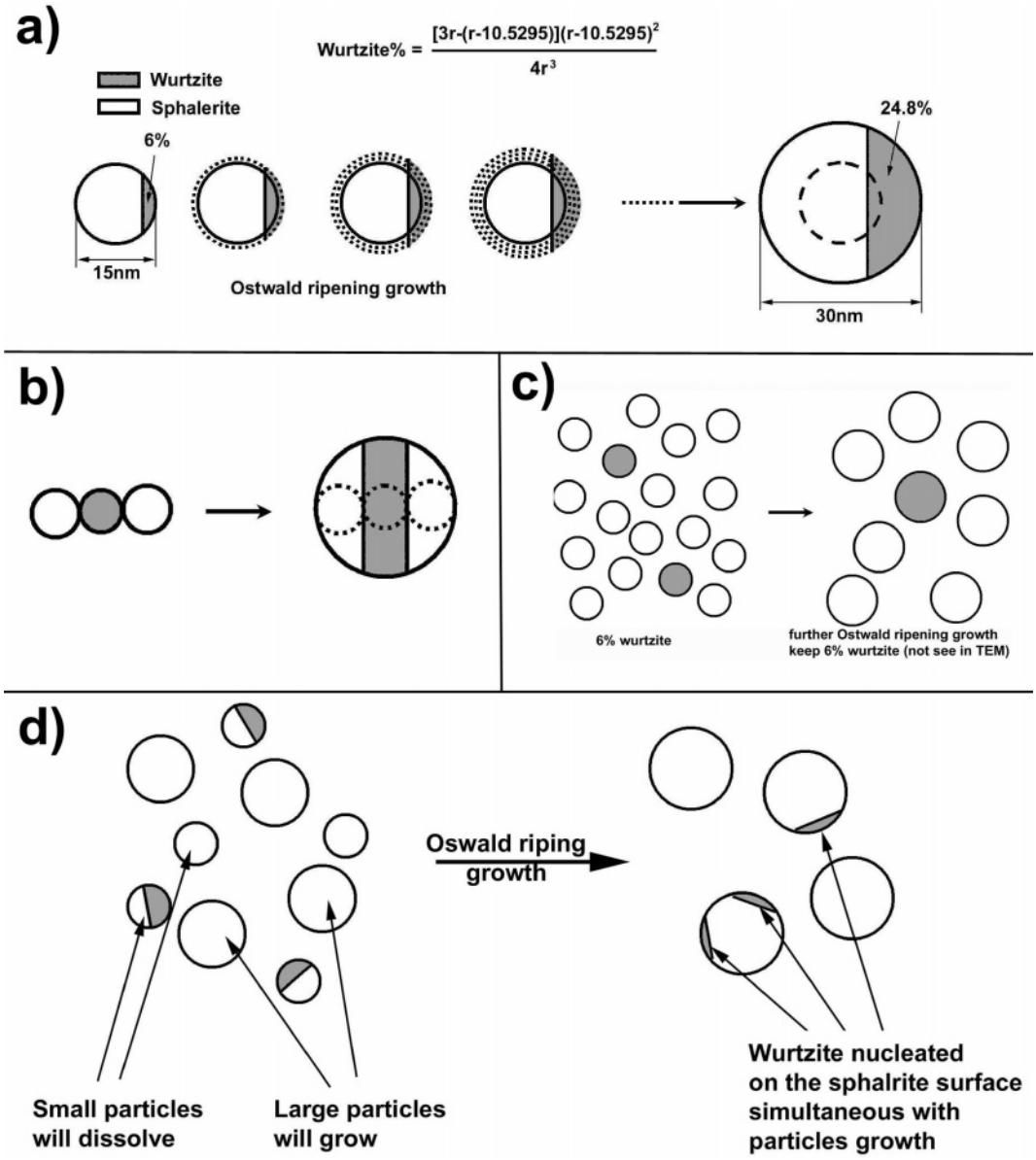

Figure 5. Illustration shows the final wurtzite microstructure detected at the end of the experiment if: (a) wurtzite formed on small particles that subsequently grew significantly via Ostwald ripening, (b) wurtzite growth occurred by OA involving wurtzite or wurtzite and sphalerite nanoparticles, or if wurtzite nucleated at twins or stacking faults within particles, (c) the initial wurtzite nuclei involved in the formation of wurtzite via Ostwald ripening, and (d) that wurtzite present at the end of the experiment nucleated on the surface of sphalerite nanoparticles after the growth phase.

sphalerite nanoparticles, or if wurtzite nucleated at twins or stacking faults within particles (Figure 5b). However, no examples of sphalerite particles containing internal wurtzite domains were found. This indicates that few wurtzite-bearing particles persisted during OA growth and that surface sites for wurtzite nucleation are significantly more energetically favorable than internal defects.

The smallest sphalerite particles within the samples should be most prone to transform to wurtzite. One mode of growth of wurtzite may be formation of wurtzite nuclei that then grow via Ostwald ripening. However, this would generate large wurtzite particles that were not detected in the sample (Figure 5c). Thus, we conclude that Wurtzite formed at the early stage dissolved in the following Ostwald ripening growth, and wurtzite present at the end of the experiment nucleated on the surface of sphalerite nanoparticles after the growth phase (Figure 5d).

The distribution of wurtzite as caps on {111} sphalerite (Figures 3 and 4) suggests transformation of sphalerite to wurtzite occurred after the particles were rounded (surface topography was removed). The consistency of the diameter of the wurtzite−sphalerite interface may indicate that a kinetic factor related to the area of the sphalerite−wurtzite interface hindered propagation of wurtzite into the sphalerite, even at long reaction times.

Typical models based on multiple defect nucleation kinetics[1,2] in bulk materials and models for single defect nucleation kinetics[5,8] in very small nanoparticles cannot explain the observed phase transformation kinetics. In the traditional models, the phase transformation kinetics are controlled by the nucleation rate at transformation temperature. Nucleation of the second phase is induced by defects, and growth is controlled by the movement of these defects through the crystals. The activation energy to form defects is usually high, whereas the energy to

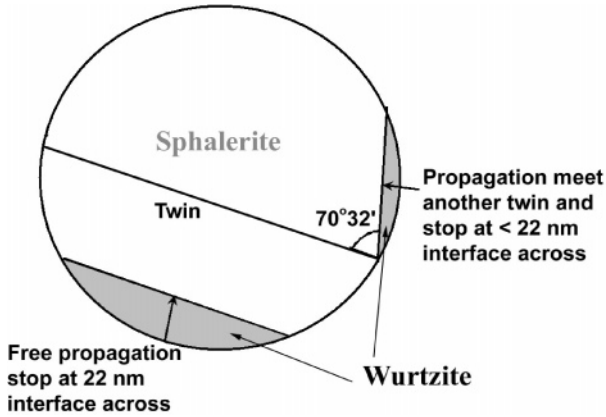

Figure 6. Illustration shows the free wurtzite propagation and wurtzite propagation meet with a nonparallel twin layer.

move defects is usually comparatively small. Thus, once a defect is formed, the boundary of the new phase should propagate until a surface or another propagating phase front is encountered (thus the product is 100% new phase). These traditional models are inconsistent with the transformation kinetics observed in nanoparticulate ZnS because they do not predict cessation of transformation at longer reaction times.

In addition to differences in the form of the reaction progress curves, nanoparticulate ZnS undergoes much more rapid phase transformation than would be expected in bulk ZnS at 225 °C. Because the reaction of sphalerite to wurtzite in bulk material is thermodynamically prohibited at 225 °C, the only comparison available is the reverse reaction (conversion of bulk metastable wurtzite to sphalerite). This transformation is too slow to be detected over reasonable reaction times at 225 °C, but it has been documented above 730 °C.[21] The relatively rapid transformation of sphalerite to wurtzite at 225 °C in nanoparticulate ZnS indicates that the phase transformation activation energy in nanoparticles is much smaller than that in bulk ZnS. Thus, we infer that the activation energy for the cubic to hexagonal phase transformation in ZnS depends on the particle size. We attribute this to a transformation mechanism in the nanoparticles that is fundamentally different to that operating in bulk ZnS.

In the long time coarsened sample, the sphalerite−wurtzite interfaces structure can be divided into two kinds: one has interface diameters of ∼22 nm and has no touching point with the other nonparallel twin layer (Figure 3a lower part and Figure 4), and the other has interface diameters of <22 nm and is touching the edge of the twin layer (Figure 3a right part). This is consistent with the inferred dependence of the activation energy upon particle size and suggests that the origin of the size dependence of reaction kinetics is related to a geometrical parameter of interface between wurtzite and sphalerite. As shown in Figure 6, if the wurtzite propagation were not met with the other twin layer (in other words, free propagation), the phase transformation stops at the maximum diameter value of ∼22 nm. In another situation, if the wurtzite propagation met the nonparallel twin layer before reaching the maximum diameter value, the propagation would stop immediately, because the nonparallel twins is a high steric factor for further propagation (keeping propagation will unavoidably create a very unstable high energy dislocation).

(21) Baars, J.; Brandt G. *J. Phys. Chem. Solids* **1973**, *34*, 905.

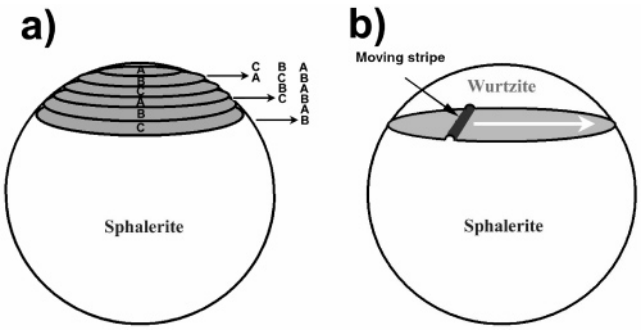

Figure 7. (a) Diagram illustrating a whole layer shift model. (b) Diagram illustrating a dislocated stripe moving in one layer.

Here we propose two simplified models to help understand the free propagation kinetics of wurtzite formation in nanocrystalline sphalerite. In these models, nucleation occurs at the surface and growth involves collective movement of atoms at the wurtzite−sphalerite interface. The first model considers interfacial area as the relevant geometric factor, whereas diameter is the key parameter in the second model.

Model 1. Sphalerite and wurtzite differ only in their close-packed stacking sequences. In the whole layer shift model, sphalerite ABCABC stacking along ⟨111⟩ converts to wurtzite ABABAB stacking along ⟨001⟩ via simultaneous displacement of entire Zn and S layers. The activation energy needed is thus proportional to the area of moving layer (interface area between sphalerite and wurtzite). For a spherical particle, the area of a layer close to the surface of a particle is much smaller than the area of layers closer to the particle center. Thus, it is much easier to shift surface layers compared to layers deeper within the particle (Figure 7a). Hence, propagation of wurtzite becomes increasingly more difficult as the interface moves toward the center of the nanoparticles.

Model 2. In this model, the change of layer sequence from ABCABC... to ABABAB... occurs by simultaneous movement of a strip of atoms across the interface. The phase transformation is localized along a defect that forms the edge of the converting layer. The defect is a single unit cell wide (0.330 nm) (see Figure 7b). The transformation of a single ZnS layer occurs via propagation of the dislocation strip across the interface. The activation energy is thus proportional to the area of the largest strip in this layer; in other words, the active energy is proportional to the diameter of the transforming layer. The larger the interface diameter is, the harder it is to transform the layer from sphalerite to wurtzite.

It is possible to construct models to describe the sets of atomic displacements that may accompany the phase transformation. Of many possible scenarios, two seem most probable (Figure 8). These models are consistent with both the layer shift and moving strip models. In the first case (Figure 8a), there is only one plane at which bonds are broken, but propagation of the interface requires that the entire cap is displaced each time the reaction front moves into the sphalerite. We do not know the magnitude of the energy penalty (if any) for simultaneous movement of the cap, and it is impossible to accurately calculate it using currently available simulation methods due to the nanoparticle size. The second model (Figure 8b) generally requires a pair of simultaneous layer shifts in opposite directions at the interface. The activation energy for this pathway would be approximately three times as large as that for a model in

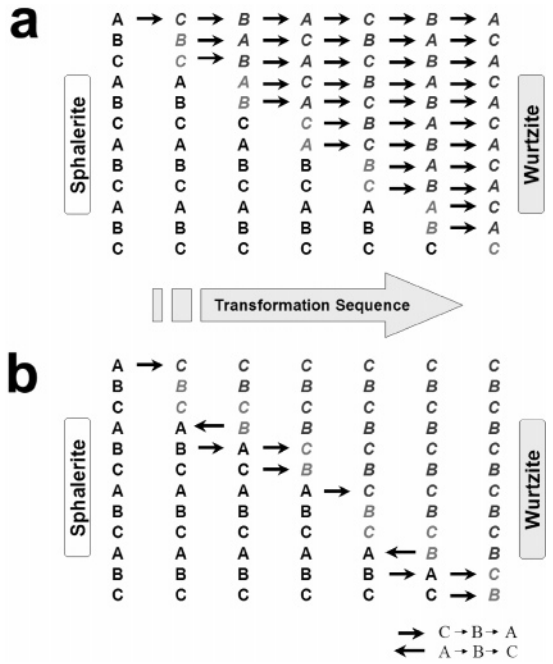

Figure 8. Two most possible atomic displacement models in the sphalerite (ABCABC... stacking series) to wurtzite (ABABAB... stacking series) phase transformation: (a) 1,3,5,7 layers move at once; only interface moved is between the cap and the underlying sphalerite; formed wurtzite cap moves as a whole part (each layer moves in one direction C → B→ A). (b) A propagating interface model; do not need the formed wurtzite cap to move as a whole part; sometimes two layers move at once in opposite direction (C → B →A and A → B → C), which may need high activation energy.

which one layer shift occurs at a time. In both cases, the energy required for the transformation will scale with the area of the interface, as described above.

Assuming the activation energy is E_a, the area of the interface or strip is S, and the kinetic constant is k, according to the Arrhenius equation:

$$k = A_0 \exp[-E_a/(RT)] \quad (2)$$

we have

$$k = A_0 \exp[-gN_0S/(RT)] \quad (3)$$

where g stands for activation energy for layer movement per unit area, N_0 is Avogadro's constant: 6.02×10^{23} mol^{-1}, T is absolute temperature 498 K, R is universal gas constant 8.314 J/(mol·K), and A_0 is the pre-exponential factor.

If the kinetic constant k becomes too small, the reaction rate becomes too slow for the phase transformation to be observed. In this discussion, we assume the phase transformation terminates at $k/A_0 \approx 10^{-6}$.[22] According to our observation, the phase transformation terminates when the interface area is ~380 nm^2, equivalent to a diameter of 22 nm. By substituting S in eq 3 with 380 nm^2 (for the whole layer shift model) or 7.26 nm^2 (=22 nm × 0.33 nm, for strip movement model), we can deduce that the activation energies per unit area (g) for transformation are around 0.29 mJ/m^2 (when $k/A_0 \approx 10^{-6}$) for transformation via whole layer shift or 15 mJ/m^2 (when $k/A_0 \approx 10^{-6}$) for the strip movement model, respectively.

It may be possible to evaluate the two models by comparing the deduced g value of each model with g values from other sources, such as from MD simulation or prior studies. However, essentially no data are available. The g value of a 30-nm particle should be between that for a 3-nm particle and that of bulk material. It should be possible to estimate the g value for bulk material and nanoparticles from existing data, and thus to infer which model more accurately describes the phase transformation process.

The concept of activation energy per unit area (g) can be extended to describe the defect-controlled phase transformation kinetics in bulk materials, given that the transformation occurs one Zn−S pair at a time. In this kinetic model, the transformation processes can be viewed as an Zn−S atom pair moving from B position to C position (Figure 9); thus the area of the moving unit, S, is the area of the base of a single cell: 0.1258 nm^2. By substituting T in eq 3 with 1003 K (730 °C, the temperature of onset of the defected induced phase transformation), we can estimate that the g value within bulk materials is 1521 mJ/m^2 (when $k/A_0 \approx 10^{-6}$). This value is about 100 and 1000 times larger than the value estimated for the whole layer shift and the strip movement models, respectively.

On surfaces of bulk materials, atomic movements are less constrained. A preliminary MD simulation (H. Zhang, personal communication) shows that, for the layers on the surface of bulk materials, g is about 60 mJ/m^2, which is about 10 times less than the value for transformation inside the crystal. As expected, this g value is much larger than the values deduced for our two models.

It is possible to constrain the value of g in very small particles using the observation that phase transformations driven by aggregation[23] and water adsorption[24] occur at appreciable rates at room temperature. Using eq 3, $k/A_0 = 10^{-6}$, and S estimated from the surface area of a 3-nm nanoparticle, we found that appreciable phase transformation should only occur if $g < \sim 2$ mJ/m^2. The g value for the 30-nm particles should be between those for the bulk material and the nanoparticles. As only the g value for the strip movement model meets this requirement, it may better describe the phase transformation mechanism.

Conclusion

Partial transformation of sphalerite to wurtzite accompanies crystal growth of ZnS nanoparticles in hydrothermal solution. The data are consistent with phase stability wurtzite at small particle size (3−7 nm) at 225 °C. Formation of wurtzite over relatively short reaction times at this temperature implies a phase transformation mechanism that differs from that operating in bulk ZnS. The transformation did not go to completion within the rounded sphalerite particles, but stopped when the diameter of the interface between sphalerite and wurtzite reached ~22 nm. We developed atomic-level models to describe the transformation mechanism and determined that collective movement of a reaction front strip across the interface is most consistent with the activation energy inferred by kinetic analysis. Accurate

(22) If we assume the reaction terminated when $k/A_0 < 10^{-6}$, then the transformation stops when the k value is less than 10^{-6} times the initial rate determined by A_0. Even if we use the more rigorous limit of $k/A_0 < 10^{-12}$, the activation energy per unit area (g) only increases by a factor of 2 relative to that determined if we assume $k/A < 10^{-6}$. Our analysis is thus only slightly sensitive to the value used to define the limit for detectable transformation.

(23) Huang, F.; Gilbert, B.; Zhang, H.; Banfield, J. F. *Phys. Rev. Lett.* **2004**, *92*, 15501.
(24) Zhang, H.; Gilbert, B.; Huang, F.; Banfield, J. F. *Nature* **2003**, *424*, 1025

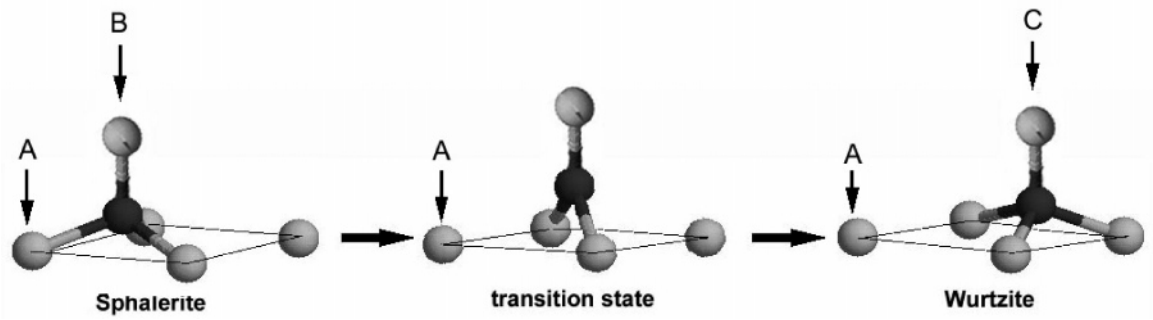

Figure 9. Diagram illustrating the transition of ZnS atom pair from B position to C position.

measurements of the activation energy for the phase transformation in bulk material and very small particles are needed for further analysis.

Acknowledgment. We thank Dr. Hengzhong Zhang and Benjamin Gilbert for helpful discussion. Financial support for this study was provided by National Science Foundation Grant EAR-9814333, the Lawrence Berkeley National Laboratory LDRD program, and the Department of Energy Basic Energy Sciences Program Grant DE-FG03-01ER15218. Transmission electron microscope characterization was conducted in the Materials Science Center, University of Wisconsin-Madison.

JA048121C